Pramana – J. Phys. (2019) 93:54
https://doi.org/10.1007/s12043-019-1809-0

Entropy generation optimisation in the nanofluid flow of a second grade fluid with nonlinear thermal radiation

TASAWAR HAYAT[1,2], MEHREEN KANWAL[1], SUMAIRA QAYYUM[1,*], M IJAZ KHAN[1] and AHMED ALSAEDI[2]

[1]Department of Mathematics, Quaid-I-Azam University 45320, Islamabad 44000, Pakistan
[2]Nonlinear Analysis and Applied Mathematics (NAAM) Research Group, Department of Mathematics, Faculty of Science, King Abdulaziz University, Jeddah 21589, Saudi Arabia
*Corresponding author. E-mail: sumaira@math.qau.edu.pk

MS received 12 February 2019; revised 13 March 2019; accepted 14 March 2019; published online 12 July 2019

Abstract. The flow of a second grade fluid by a rotating stretched disk is considered. Brownian motion and thermophoresis characterise the nanofluid. Entropy generation in the presence of heat generation/absorption, Joule heating and nonlinear thermal radiation is discussed. Homotopic convergent solutions are developed. The behaviour of velocities (radial, axial, tangential), temperature, entropy generation, Bejan number, Nusselt number, skin friction and concentration is evaluated. The radial, axial and tangential velocities increase for larger viscoelastic parameters while the opposite trend is noted for temperature. Concentration decreases when Schmidt number and Brownian diffusion increase. Entropy generation increases when the Bejan number increase while the opposite is true for the Brinkman number and the magnetic parameter.

Keywords. Buongiorno model; entropy generation; heat generation/absorption; Joule heating; nonlinear thermal radiation; second grade fluid.

PACS Nos 47.10.A; 47.15.G; 47.27.Ak

1. Introduction

The requirements for the development in the heat transfer rate cannot be achieved by ordinary fluids like water, kerosene oil, ethylene glycol, etc. Several experiments have been carried out by the researchers for improving heat exchange. Many techniques have been proposed in this direction by enhancing micrometre-sized particles for the thermal conductivity of conventional fluids. The major drawbacks in heat transfer components and high-pressure drops are blockage and erosion. To overcome such issues, the idea of nanofluids is introduced. Nanofluids is a suspension of particles of size 1–100 nm in base fluids. It is very effective as the suspension of these particles can enhance the thermal conductivity of base fluids and thus is useful in increasing the heat transfer rate. The enhancement of the thermophysical properties of conventional fluids using nanoparticles suspension is first examined by Choi [1]. Nanofluids have many applications in fields such as nanocryosurgery, environment engineering, chemical industry, heat control systems, heat exchangers, energy storage, power production, refrigeration process, etc. Due to these noteworthy applications, many researchers have already worked on this topic [1–10]. Many materials in nature have diverse properties. All such materials cannot be handled by the Navier–Stokes theory. These materials are viscoelastic. Food stuff, care products, ketchup, shampoo, many fuel and oils are a few examples of such fluids. Many models like Maxwell, Williamson, Sisko, Jeffrey, Oldroyd-B, Burgers, generalised Burgers, etc. are developed for describing these fluids. Some contributions in this direction have already been made [11–19].

The irreversibility process in the system is called entropy. In thermodynamics, the transfer of heat is related to the minimum change of entropy. To enhance the ability of machines, entropy generation minimisation (EGM) is utilised. Some applications of EGM include spin moment, internal molecular friction, kinetic energy and vibration. This type of loss of energy cannot be regained without extra work. That is why entropy is called the measure of irreversibility through heat transfer, mass transfer or viscous dissipation. Several scientists used this process of minimisation in many systems like natural convection, fuel cells,

cooling by evaporation, gas turbines, etc. Qayyum *et al* [20] analysed entropy generation in radiative and Von Karman's swirling flow with Soret and Dufour effects. Berdichevsky [21] studied the effect of crystal plasticity in the presence of entropy. Khan *et al* [22] worked on disorderedness of the system for nanofluid flow after considering Arrhenius activation energy. An increase in the efficiency of thermal power plants through entropy generation is examined by Haseli [23]. Hayat *et al* [24] discussed the entropy generation of a flow with nonlinear thermal radiation. The generation of entropy in a gaseous phosphorus dimer is discussed by Jia *et al* [25]. The simulation of entropy generation by a similar method can be seen in [25] and Gibbs free energy and enthalpy generation in nitrogen monoxide and gaseous phosphorus dimer can be seen in refs [26–28].

This paper examines entropy generation optimisation for the flow of a second-grade nanofluid. Nonlinear thermal radiation, heat generation/absorption and Joule heating in formulation are considered. The relevant nonlinear problems are computed for the convergent series solutions by the homotopy analysis method [7,29–35]. The effects of sundry variables on velocity, temperature, Bejan number, entropy generation, skin friction coefficients and concentration are examined.

2. Formulation

The flow of a second-grade nanofluid by a stretchable rotating disk is examined. Entropy generation for viscous dissipation, Joule heating and nonlinear thermal radiation is also discussed. A magnetic field of constant strength (B_0) is exerted in the z-direction. The disk at $z = 0$ rotates at an angular velocity (Ω_1) (see figure 1). The stretching velocity of the disk is a (with a being the stretching rate). The disk and ambient temperature are denoted by $\hat{T}_w$ and $\hat{T}_\infty$, respectively. The surface and ambient concentrations are $\hat{C}_w$ and $\hat{C}_\infty$.

The governing equations in component form are

$$\frac{\partial \hat{w}}{\partial z} + \frac{\hat{u}}{r} + \frac{\partial \hat{u}}{\partial r} = 0, \tag{1}$$

$$\frac{\partial \hat{u}}{\partial z}\hat{w} - \frac{\hat{v}^2}{r} + \frac{\partial \hat{u}}{\partial r}\hat{u} = \frac{\alpha_1}{\rho_f}\left(\begin{array}{l} \dfrac{\partial^3 \hat{u}}{\partial r \partial z^2}\hat{u} - \dfrac{1}{r}\left(\dfrac{\partial \hat{u}}{\partial z}\right)^2 + 2\dfrac{\partial \hat{u}}{\partial r}\dfrac{\partial^2 \hat{u}}{\partial z^2} \\ \dfrac{\partial^3 \hat{u}}{\partial z^3}\hat{w} + \dfrac{\partial \hat{v}}{\partial r}\dfrac{\partial^2 \hat{v}}{\partial z^2} + \dfrac{\partial^2 \hat{u}}{\partial z^2}\dfrac{\partial \hat{w}}{\partial z} \\ \quad + \dfrac{\partial \hat{v}}{\partial z}\dfrac{\partial^2 \hat{v}}{\partial r \partial z} + 3\dfrac{\partial \hat{u}}{\partial z}\dfrac{\partial^2 \hat{u}}{\partial r \partial z} - \dfrac{\partial^2 \hat{v}}{\partial z^2}\dfrac{\hat{v}}{r} \end{array}\right)$$

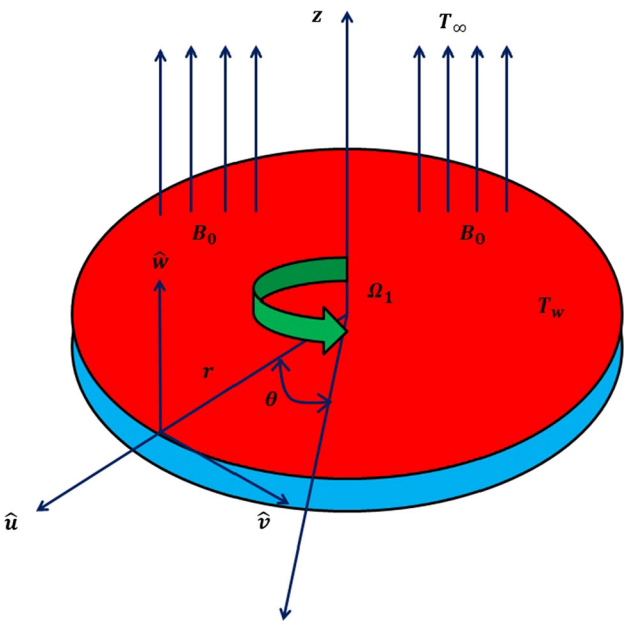

Figure 1. Flow geometry.

$$+\nu_f \frac{\partial^2 \hat{u}}{\partial z^2} - \frac{\sigma_f B_0^2}{\rho_f}\hat{u}, \tag{2}$$

$$\frac{\partial \hat{v}}{\partial z}\hat{w} + \frac{\partial \hat{v}}{\partial r}\hat{u} + \frac{\hat{v}\hat{u}}{r} = \frac{\alpha_1}{\rho_f}\left(\begin{array}{l} \dfrac{\partial^2 \hat{v}}{\partial z^2}\dfrac{\hat{u}}{r} - 2\dfrac{\partial \hat{v}}{\partial z}\dfrac{\partial^2 \hat{u}}{\partial r \partial z} \\ \dfrac{\partial^3 \hat{v}}{\partial r \partial z^2}\hat{u} + \dfrac{\partial^3 \hat{v}}{\partial z^3}\hat{w} - \dfrac{1}{r}\dfrac{\partial \hat{u}}{\partial z}\dfrac{\partial \hat{v}}{\partial z} \end{array}\right) + \nu_f \frac{\partial^2 \hat{v}}{\partial z^2} - \frac{\sigma_f B_0^2}{\rho_f}\hat{v}, \tag{3}$$

$$\begin{aligned} &(\rho c_p)_f\left(\frac{\partial \hat{T}}{\partial z}\hat{w} + \frac{\partial \hat{T}}{\partial r}\hat{u}\right) \\ &= k_f \frac{\partial^2 \hat{T}}{\partial z^2} + Q^*(\hat{T} - \hat{T}_\infty) \\ &\quad + \sigma_f B_0^2(\hat{v}^2 + \hat{u}^2) \\ &\quad - \frac{16\sigma^*}{3k^*}\left[\hat{T}^3\frac{\partial^2 \hat{T}}{\partial z^2} + 3\hat{T}^2\left(\frac{\partial \hat{T}}{\partial z}\right)^2\right] \\ &\quad + (\rho c_p)_s\left[\frac{D_T}{T_\infty}\left(\frac{\partial \hat{T}}{\partial z}\right)^2 + D_B\left(\frac{\partial \hat{T}}{\partial z}\frac{\partial \hat{C}}{\partial z}\right)\right], \end{aligned} \tag{4}$$

$$\frac{\partial \hat{C}}{\partial r}\hat{u} + \frac{\partial \hat{C}}{\partial z}\hat{w} = D_B\frac{\partial^2 \hat{C}}{\partial z^2} + \frac{D_T}{T_\infty}\left(\frac{\partial^2 \hat{T}}{\partial z^2}\right), \tag{5}$$

with boundary conditions

$$\hat{u} = ra, \quad \hat{v} = r\Omega_1, \quad \hat{w} = 0,$$

$$\hat{C} = \hat{C}_w, \quad \hat{T} = \hat{T}_w, \quad \hat{p} \to 0 \text{ at } z = 0,$$
$$\hat{u} = 0, \quad \hat{v} = 0, \quad \hat{C} \to \hat{C}_\infty$$
$$\hat{T} = \hat{T}_\infty \text{ when } z \to \infty. \tag{6}$$

Here $(\hat{u}, \hat{v}, \hat{w})$ are velocities in the $(\hat{r}, \hat{\theta}, \hat{z})$ directions of the disk, α_1 is the material parameter, ν_f is the kinematic viscosity, ρ_f is the density, $\hat{p}$ is the pressure, k_f is the thermal conductivity, c_p is the specific heat, Q^* is the heat generation/absorption coefficient and D_B is the coefficient of diffusion species. Considering [18]

$$\hat{u} = r\Omega_1 \tilde{f}'(\xi), \quad \hat{v} = r\Omega_1 \tilde{g}(\xi), \quad \tilde{w} = -2h\Omega_1 \tilde{f}(\xi),$$
$$\hat{\varphi} = \frac{\hat{C} - \hat{C}_\infty}{\hat{C}_w - \hat{C}_\infty}, \quad \hat{\theta} = \frac{\hat{T} - \hat{T}_\infty}{\hat{T}_w - \hat{T}_\infty},$$
$$\hat{p} = \rho_f \Omega_1 \nu_f \left(P(\xi) + \frac{1}{2}\frac{r^2}{h^2}\varepsilon \right), \quad \xi = \frac{z}{h}, \tag{7}$$

the continuity equation is satisfied and eqs (2)–(6) are reduced in the dimensionless form as

$$\tilde{f}''' + \text{We Re}\left(2\tilde{f}''^2 + \tilde{g}'^2 - 2\tilde{f}\tilde{f}^{(iv)} + \tilde{f}'\tilde{f}'''\right) - \text{Re}\left(\tilde{f}'^2 - 2\tilde{f}\tilde{f}'' - \tilde{g}^2\right) - M\tilde{f}' = 0, \tag{8}$$

$$\tilde{g}'' + \text{We Re}\left(2f'\tilde{g}'' - 2\tilde{f}\tilde{g}''' - 3\tilde{f}''\tilde{g}'\right) - \text{Re}\left(2\tilde{f}'\tilde{g} - 2\tilde{f}\tilde{g}'\right) - M\tilde{g} = 0, \tag{9}$$

$$\tilde{\theta}'' + 2\text{Re Pr}\, \tilde{f}\tilde{\theta}' + \text{Re Pr}\, Q\tilde{\theta} + N_\text{b}\,\text{Pr}\,\tilde{\theta}'\tilde{\varphi}' + N_\text{t}\,\text{Pr}\tilde{\theta}'^2 + R_d\left(3(\theta_w - 1)\left(\tilde{\theta}'^2 + \tilde{\theta}^2\tilde{\theta}'^2(\theta_w - 1)^2 + 2\tilde{\theta}\tilde{\theta}'^2(\theta_w - 1)\right) + \tilde{\theta}'' + (\theta_w - 1)^3\tilde{\theta}^3\tilde{\theta}'' + 3(\theta_w - 1)\tilde{\theta}\tilde{\theta}'' + 3(\theta_w - 1)^2\tilde{\theta}^2\tilde{\theta}''\right) + M\,\text{Pr}\,\text{Ec}\left(\tilde{f}'^2 + \tilde{g}^2\right) = 0, \tag{10}$$

$$\tilde{\varphi}'' + 2\text{Re Sc}\,\tilde{f}\tilde{\varphi}' + \frac{N_\text{t}}{N_\text{b}}\tilde{\theta}'' = 0 \tag{11}$$

with

$$\tilde{f}(0) = 0, \ \tilde{f}'(0) = A, \ \tilde{f}'(\infty) = 0, \ \tilde{g}(0) = 1, \ \tilde{g}(\infty) = 0, \ \tilde{\theta}(0) = 1, \ \tilde{\theta}(\infty) = 0, \ \tilde{\varphi}(0) = 1, \ \tilde{\varphi}(\infty) = 0, \ p(0) = 0, \tag{12}$$

where

$$\text{We} = \frac{\alpha_1}{\rho h^2}, \quad \text{Re} = \frac{\Omega_1 h^2}{\nu_f}, \quad \text{Pr} = \frac{(\rho c_p)_f \nu_f}{k_f},$$
$$A = \frac{a}{\Omega_1}, \quad Q = \frac{Q^*}{\rho c_p \Omega_1}, \quad \text{Sc} = \frac{\upsilon}{Dc^*},$$
$$\delta = \frac{D_d^*}{Dc^*}, \quad N_\text{b} = \frac{\tau D_B (C_w - C_\infty)}{\upsilon},$$
$$N_\text{t} = \frac{\tau D_B (T_w - T_\infty)}{T_\infty \upsilon}, \quad M = \frac{\sigma B_0^2}{\rho\Omega_1},$$
$$R_d = \frac{16\sigma^* T_\infty^3}{3k_f pk^*},$$
$$\theta_w = \frac{T_w}{T_\infty}, \quad \text{Ec} = \frac{r^2\Omega_1^2}{c_p(T_w - T_\infty)}, \tag{13}$$

in which We, Re, Pr, A, Q, Sc, δ, N_b, N_t, M, R_d, θ_w and Ec represent the Weissenberg number, Reynolds number, Prandtl number, stretching parameter, heat generation/absorption parameter, Schmidt number, ratio of diffusion coefficient, Brownian parameter, thermophoresis parameter, magnetic parameter, radiation parameter, temperature difference and the Eckert number, respectively.

We have $C_{f\theta}$ and C_{fr} as skin friction coefficients in the tangential and radial direction, i.e.

$$\left.\begin{aligned} C_{f\theta} &= \frac{\tau_{zr}}{\rho(r\Omega_1)^2} \\ C_{fr} &= \frac{\tau_{z\theta}}{\rho(r\Omega_1)^2} \end{aligned}\right\}, \tag{14}$$

where shear stresses τ_{zr} and $\tau_{z\theta}$ are

$$\begin{aligned} \tau_{zr} = \mu\left(\frac{\partial\hat{w}}{\partial r} + \frac{\partial\hat{u}}{\partial z}\right) + \alpha_1\Bigg[&+2\left(\frac{\partial\hat{v}}{\partial r} - \frac{\hat{v}}{r}\right)\frac{\partial\hat{v}}{\partial z} \\ &+\left(\frac{\partial\hat{u}}{\partial z} + \frac{\partial\hat{w}}{\partial r}\right)\left(\frac{\partial}{\partial r}\hat{u} + \frac{\partial}{\partial z}\hat{w}\right) \\ &+\frac{\partial\hat{w}}{\partial z}\frac{\partial\hat{u}}{\partial z} + \frac{\partial\hat{u}}{\partial r}\frac{\partial\hat{w}}{\partial r} + 3\left(\frac{\partial\hat{w}}{\partial r}\frac{\partial\hat{w}}{\partial z} + \frac{\partial\hat{u}}{\partial z}\frac{\partial\hat{u}}{\partial r}\right)\Bigg] \\ &-\alpha_1\Bigg(\left(\frac{\partial\hat{v}}{\partial r} - \frac{\hat{v}}{r}\right)\frac{\partial\hat{v}}{\partial z} \\ &+\left(\frac{\partial\hat{u}}{\partial r} + \frac{\partial\hat{w}}{\partial z}\right)\left(\frac{\partial\hat{u}}{\partial z} + \frac{\partial\hat{w}}{\partial r}\right)\Bigg), \end{aligned} \tag{15}$$

$$\begin{aligned} \tau_{z\theta} = \mu\frac{\partial\hat{v}}{\partial z} + \alpha_1\Bigg(&\frac{\partial^2 v}{\partial z^2}\hat{w} - \frac{\hat{v}}{r}\frac{\partial\hat{u}}{\partial z} + \frac{\partial\hat{v}}{\partial z}\frac{\partial\hat{w}}{\partial z} \\ &+\frac{\partial^2\hat{v}}{\partial r\partial z}\hat{u} + \frac{\partial\hat{u}}{\partial z}\frac{\partial\hat{v}}{\partial r} + 3\frac{\hat{u}}{r}\frac{\partial\hat{v}}{\partial z}\Bigg) \\ &-\alpha_1\Bigg(\frac{\partial\hat{u}}{\partial z}\frac{\partial\hat{v}}{\partial r} + 2\frac{\hat{u}}{r}\frac{\partial\hat{v}}{\partial z} + 2\frac{\partial\hat{v}}{\partial z}\frac{\partial\hat{w}}{\partial z} - \frac{\hat{v}}{r}\frac{\partial\hat{w}}{\partial r} \\ &-\frac{\hat{v}}{r}\frac{\partial\hat{u}}{\partial z} + \frac{\partial\hat{w}}{\partial r}\frac{\partial\hat{v}}{\partial r}\Bigg). \end{aligned} \tag{16}$$

Skin friction coefficients in the dimensionless form are

$$\text{Re}_r\, C_{fr} = \tilde{f}''(0) + \text{We Re}\left(3\tilde{f}'(0)\tilde{f}''(0) - 2\tilde{f}(0)\tilde{f}'''(0)\right), \tag{17}$$

$$\mathrm{Re}_r\, C_{f\theta} = \tilde{g}'(0) + \mathrm{We}\,\mathrm{Re}\big(4\tilde{f}'(0)\tilde{g}'(0) - 2\tilde{f}(0)\tilde{g}''(0)\big), \tag{18}$$

where $\mathrm{Re}_r = r\Omega_1 h/\nu$ depicts the local Reynolds number.

The heat transfer rate is

$$\mathrm{Nu}_x = \frac{hq_w}{k(\hat{T}_w - \hat{T}_\infty)}. \tag{19}$$

The wall heat flux (q_w) is defined as

$$q_w|_{z=0} = -k\frac{\partial \hat{T}}{\partial z}\bigg|_{z=0} - \frac{16\sigma^*\hat{T}^3}{3k^*}\frac{\partial \hat{T}}{\partial z}\bigg|_{z=0}. \tag{20}$$

The Nusselt number in the dimensionless form is

$$\mathrm{Nu}_x = -\tilde{\theta}'(0)\big(1 + R_d\theta_w^3\big). \tag{21}$$

2.1 *Entropy generation*

Entropy generation in the nanofluid flow of a second-grade fluid with nonlinear thermal radiation irreversibility, viscous dissipation irreversibility and Joule heating irreversibility is discussed here. The dimensional form is defined as

$$S_G = \frac{k_f}{\hat{T}_\infty^2}\left[1 + \frac{16\sigma^*\hat{T}^3}{3k_f k^*}\right]\left(\frac{\partial \hat{T}}{\partial z}\right)^2 + \frac{\Phi}{\hat{T}_\infty} + \frac{\sigma_f}{\hat{T}_\infty}B_0^2\big(\hat{v}^2 + \hat{u}^2\big) + \frac{RD}{\hat{T}_\infty}\left(\frac{\partial \hat{T}}{\partial z}\frac{\partial \hat{C}}{\partial z}\right) + \frac{RD}{\hat{C}_\infty}\left(\frac{\partial \hat{C}}{\partial z}\right)^2, \tag{22}$$

where

$$\Phi = \mu_f\left[\left(\frac{\partial \hat{u}}{\partial z}\right)^2 + \left(\frac{\partial \hat{v}}{\partial z}\right)^2\right] + \alpha_1\left[-\frac{\hat{v}}{r}\frac{\partial \hat{v}}{\partial z}\frac{\partial \hat{u}}{\partial z} - \frac{\partial \hat{v}}{\partial r}\frac{\partial \hat{v}}{\partial z}\frac{\partial \hat{u}}{\partial z} + 2\frac{\partial \hat{u}}{\partial r}\left(\frac{\partial \hat{u}}{\partial z}\right)^2 + \hat{u}\frac{\partial \hat{u}}{\partial z}\frac{\partial^2 \hat{u}}{\partial r\partial z} + \frac{\partial \hat{w}}{\partial z}\left(\frac{\partial \hat{u}}{\partial z}\right)^2 + \hat{w}\frac{\partial \hat{v}}{\partial z}\frac{\partial^2 \hat{v}}{\partial z^2} + \frac{\hat{v}}{r}\left(\frac{\partial \hat{u}}{\partial z}\right)^2 - \frac{\partial \hat{v}}{\partial r}\left(\frac{\partial \hat{u}}{\partial z}\right)^2\right]. \tag{23}$$

The above two equations yield

$$S_G = \frac{k_f}{\hat{T}_\infty^2}\left[1 + \frac{16\sigma^*\hat{T}^3}{3k_f k^*}\right]\left(\frac{\partial \hat{T}}{\partial z}\right)^2 + \frac{1}{\hat{T}_\infty}\left[\mu_f\left[\left(\frac{\partial \hat{u}}{\partial z}\right)^2 + \left(\frac{\partial \hat{v}}{\partial z}\right)^2\right] + \alpha_1\left[2\frac{\partial \hat{u}}{\partial r}\left(\frac{\partial \hat{u}}{\partial z}\right)^2 - \frac{\hat{v}}{r}\frac{\partial \hat{v}}{\partial z}\frac{\partial \hat{u}}{\partial z} - \frac{\partial \hat{v}}{\partial r}\frac{\partial \hat{v}}{\partial z}\frac{\partial \hat{u}}{\partial z} + \hat{u}\frac{\partial \hat{u}}{\partial z}\frac{\partial^2 \hat{u}}{\partial r\partial z}\right] + \hat{w}\frac{\partial \hat{v}}{\partial z}\frac{\partial^2 \hat{v}}{\partial z^2} + \frac{\partial \hat{w}}{\partial z}\left(\frac{\partial \hat{u}}{\partial z}\right)^2 - \frac{\partial \hat{v}}{\partial r}\left(\frac{\partial \hat{u}}{\partial z}\right)^2 + \frac{\hat{v}}{r}\left(\frac{\partial \hat{u}}{\partial z}\right)^2\right] + \frac{\sigma_f}{\hat{T}_\infty}B_0^2\big(\hat{u}^2 + \hat{v}^2\big) + \frac{RD}{\hat{C}_\infty}\left(\frac{\partial \hat{C}}{\partial z}\right)^2 + \frac{RD}{\hat{T}_\infty}\left(\frac{\partial \hat{T}}{\partial z}\frac{\partial \hat{C}}{\partial z}\right). \tag{24}$$

Equation (24) consists of four factors: (i) heat transfer irreversibility, (ii) fluid friction irreversibility, (iii) Joule heating irreversibility and (iv) diffusive irreversibility. Now, eq. (24) in the dimensionless form is

$$N_G = \alpha_1\big[1 + R_d\big(1 + \tilde{\theta}\big(\theta_w - 1\big)\big)^3\big]\tilde{\theta}'^2 + \mathrm{Br}\big(\tilde{f}''^2 + \tilde{g}'^2\big) + \mathrm{We}\,\mathrm{Re}\,\mathrm{Br}\big(\tilde{f}'\tilde{f}''^2 - 2\tilde{f}''\tilde{g}\tilde{g}' - 2\tilde{f}\tilde{g}'\tilde{g}''\big) + \mathrm{Br}M\big(\tilde{f}'^2 + \tilde{g}^2\big) + L^*\tilde{\theta}'\tilde{\varphi}' + L^*\frac{\alpha_2}{\alpha_1}\tilde{\varphi}'^2, \tag{25}$$

in which the dimensionless parameters are

$$N_G = \frac{S_G\hat{T}_\infty h^2}{(\hat{T}_w - \hat{T}_\infty)k_f}, \quad L^* = \frac{\mathrm{RD}(\hat{C}_w - \hat{C}_\infty)}{k_f}, \quad \alpha_1 = \frac{\hat{T}_w - \hat{T}_\infty}{\hat{T}_\infty}, \alpha_2 = \frac{\hat{C}_w - \hat{C}_\infty}{\hat{C}_\infty}, \quad \mathrm{Br} = \frac{\mu_f r^2\Omega_1^2}{k_f(\hat{T}_w - \hat{T}_\infty)}, \tag{26}$$

where N_G indicates entropy generation, Br is the Brinkman number, α_1 is the temperature ratio, α_2 is the concentration ratio and L^* is the diffusive parameter. The Bejan number is defined as

$$\mathrm{Be} = \frac{\text{Entropy generation due to heat and mass transfer irreversibility}}{\text{Total entropy generation}}, \tag{27}$$

$$\mathrm{Be} = \frac{\alpha_1[1+R_d(1+\tilde{\theta}(\theta_w-1))^3]\tilde{\theta}'^2 + L^*\tilde{\theta}\tilde{\varphi}' + L^*(\alpha_2/\alpha_1)\tilde{\varphi}'^2}{\left[\begin{array}{l}\alpha_1[1+R_d(1+\tilde{\theta}(\theta_w-1))^3]\tilde{\theta}'^2 + \mathrm{Br}(\tilde{f}+\tilde{g}'^2)+\mathrm{We\,Re\,Br}(\tilde{f}'\tilde{f}''^2 - 2\tilde{f}''\tilde{g}\tilde{g}' \\ -2\tilde{f}\tilde{g}'\tilde{g}'') + \mathrm{Br}M(\tilde{f}'^2+\tilde{g}^2) + L^*\tilde{\theta}'\tilde{\varphi}' + L^*(\alpha_2/\alpha_1)\tilde{\varphi}'^2\end{array}\right]}. \tag{28}$$

3. Homotopic solutions

3.1 *Zeroth-order deformation equations*

The required linear operators and initial guesses are defined as

$$\tilde{f}_0(\xi) = (1-\exp(-\xi))A,\ \tilde{g}_0(\xi) = \exp(-\xi),$$
$$\tilde{\theta}_0(\xi) = \exp(-\xi),\ \tilde{\varphi}_0(\xi) = \exp(-\xi), \tag{29}$$

$$\mathbf{L}_{\tilde{f}}(\tilde{f}) = \tilde{f}''' - \tilde{f}',\quad \mathbf{L}_{\tilde{g}}(\tilde{g}) = \tilde{g}'' - \tilde{g},$$
$$\mathbf{L}_{\tilde{\theta}}(\tilde{\theta}) = \tilde{\theta}'' - \tilde{\theta},\quad \mathbf{L}_{\tilde{\varphi}}(\tilde{\varphi}) = \tilde{\varphi}'' - \tilde{\varphi} \tag{30}$$

with

$$\mathbf{L}_{\tilde{f}}(\tilde{f})\left[c_1 + c_2\mathrm{e}^{-\xi} + c_3\mathrm{e}^{\xi}\right] = 0,$$
$$\mathbf{L}_{\tilde{g}}(\tilde{g})\left[c_4\mathrm{e}^{-\xi} + c_5\mathrm{e}^{\xi}\right] = 0,$$
$$\mathbf{L}_{\tilde{\theta}}(\tilde{\theta})\left[c_6\mathrm{e}^{-\xi} + c_7\mathrm{e}^{\xi}\right] = 0,$$
$$\mathbf{L}_{\tilde{\varphi}}(\tilde{\varphi})\left[c_8\mathrm{e}^{-\xi} + c_9\mathrm{e}^{\xi}\right] = 0, \tag{31}$$

where $c_i\ \ (i = 1-9)$ are constants.

If $q \in [0,1]$ and ($\hbar_{\tilde{f}}$, $\hbar_{\tilde{g}}$, $\hbar_{\tilde{\theta}}$ and $\hbar_{\tilde{\varphi}}$) are the auxiliary parameters, then the zeroth-order deformation problems are

$$(1-q)\mathbf{L}_{\tilde{f}}\left\{\tilde{f}(\xi,q) - \tilde{f}_0(\xi)\right\} = q\hbar_{\tilde{f}}\mathbf{N}_{\tilde{f}}\left\{\tilde{f}(\xi,q),\ \tilde{g}(\xi,q)\right\}, \tag{32}$$

$$(1-q)\mathbf{L}_{\tilde{g}}\{\tilde{g}(\xi,q) - \tilde{g}_0(\xi)\} = q\hbar_{\tilde{g}}\mathbf{N}_{\tilde{g}}\left\{[\tilde{g}(\xi,q),\ \tilde{f}(\xi,q)\right\}, \tag{33}$$

$$(1-q)\mathbf{L}_{\tilde{\theta}}\left\{\tilde{\theta}(\xi,q) - \tilde{\theta}_0(\xi)\right\} = q\hbar_{\tilde{\theta}}\mathbf{N}_{\tilde{\theta}}\left\{\tilde{\theta}(\xi,q), \tilde{f}(\xi,q), \tilde{g}(\xi,q), \tilde{\varphi}(\xi,q)\right\}, \tag{34}$$

$$(1-q)\mathbf{L}_{\tilde{\varphi}}\{\tilde{\varphi}(\xi,q) - \tilde{\varphi}_0(\xi)\} = q\hbar_{\tilde{\varphi}}\mathbf{N}_{\tilde{\varphi}}\left\{\tilde{\varphi}(\xi,q), \tilde{f}(\xi,q), \tilde{\theta}(\xi,q)\right\}, \tag{35}$$

$$\tilde{f}(0,q) = 0,\quad \tilde{f}'(0,q) = A,\quad \tilde{f}'(\infty,q) = 0, \tag{36}$$

$$\tilde{g}(0,q) = 1,\quad \tilde{g}'(0,q) = 0, \tag{37}$$

$$\tilde{\theta}(0,q) = 1,\quad \tilde{\theta}(\infty,q) = 0, \tag{38}$$

$$\tilde{\varphi}(0,q) = 1,\quad \tilde{\varphi}(\infty,q) = 0 \tag{39}$$

with operators $\mathbf{N}_{\tilde{f}}$, $\mathbf{N}_{\tilde{g}}$, $\mathbf{N}_{\tilde{\theta}}$ and $\mathbf{N}_{\tilde{\varphi}}$ in the forms

$$\begin{aligned}\mathbf{N}_{\tilde{f}} = {} & \frac{\partial^3\tilde{f}(\xi,q)}{\partial\xi^3} + \mathrm{We\,Re}\left(2\left(\frac{\partial^2\tilde{f}(\xi,q)}{\partial\xi^2}\right)^2\right. \\ & + \left(\frac{\partial\tilde{g}(\xi,q)}{\partial\xi}\right)^2 - 2\tilde{f}(\xi,q)\frac{\partial^4\tilde{f}(\xi,q)}{\partial\xi^4} \\ & \left. + \frac{\partial\tilde{f}(\xi,q)}{\partial\xi}\frac{\partial^3\tilde{f}(\xi,q)}{\partial\xi^3}\right) \\ & - \mathrm{Re}\left[\left(\frac{\partial\tilde{f}(\xi,q)}{\partial\xi}\right)^2 - 2\tilde{f}(\xi,q)\frac{\partial^2\tilde{f}(\xi,q)}{\partial\xi^2}\right. \\ & \left. - (\tilde{g}(\xi,q))^2\right] - M\frac{\partial\tilde{f}(\xi,q)}{\partial\xi},\end{aligned} \tag{40}$$

$$\begin{aligned}\mathbf{N}_{\tilde{g}} = {} & \frac{\partial^2\tilde{g}(\xi,q)}{\partial\xi^2} + \mathrm{We\,Re}\left(2\frac{\partial\tilde{f}(\xi,q)}{\partial\xi}\frac{\partial^2\tilde{g}(\xi,q)}{\partial\xi^2}\right. \\ & \left. - 2\tilde{f}(\xi,q)\frac{\partial^3\tilde{g}(\xi,q)}{\partial\xi^3} - 3\frac{\partial^2\tilde{f}(\xi,q)}{\partial\xi^2}\frac{\partial\tilde{g}(\xi,q)}{\partial\xi}\right) \\ & - \mathrm{Re}\left(2\frac{\partial\tilde{f}(\xi,q)}{\partial\xi}\tilde{g}(\xi,q) - 2\tilde{f}(\xi,q)\frac{\partial\tilde{g}(\xi,q)}{\partial\xi}\right) \\ & - M\tilde{g}(\xi,q),\end{aligned} \tag{41}$$

$$\begin{aligned}\mathbf{N}_{\tilde{\theta}} = {} & \frac{\partial^2\tilde{\theta}(\xi,q)}{\partial\xi^2} + 2\mathrm{Re\,Pr}\tilde{f}(\xi,q)\frac{\partial\tilde{\theta}(\xi,q)}{\partial\xi} \\ & + \mathrm{Re\,Pr}Q\tilde{\theta}(\xi,q) \\ & + N_{\mathrm{t}}\mathrm{Pr}\left(\frac{\partial\tilde{\theta}(\xi,q)}{\partial\xi}\right)^2 + N_{\mathrm{b}}\mathrm{Pr}\frac{\partial\tilde{\theta}(\xi,q)}{\partial\xi}\frac{\partial\tilde{\varphi}(\xi,q)}{\partial\xi} \\ & + M\mathrm{Pr\,Ec}\left\{\left(\frac{\partial\tilde{f}(\xi,q)}{\partial\xi}\right)^2 + (\tilde{g}(\xi,q))^2\right\} \\ & + R_d\left\{3(\theta_w-1)\left(\frac{\partial\tilde{\theta}(\xi,q)}{\partial\xi}\right)^2\right. \\ & \left.\times\left[1+\left(\tilde{\theta}(\xi,q)\right)^2(\theta_w-1)^2 + 2\tilde{\theta}(\xi,q)(\theta_w-1)\right]\right.\end{aligned}$$

$$+\frac{\partial^2\tilde{\theta}(\xi,q)}{\partial\xi^2}\Big[1+(\theta_w-1)^3(\tilde{\theta}(\xi,q))^3 +3(\theta_w-1)^2(\tilde{\theta}(\xi,q))^2+3(\theta_w-1)\tilde{\theta}(\xi,q)\Big]\Big\}, \tag{42}$$

$$\mathbf{N}_{\tilde{\varphi}}=\frac{\partial^2\tilde{\varphi}(\xi,q)}{\partial\xi^2}+2\mathrm{Sc}\ \mathrm{Re}\ \tilde{f}(\xi,q)\frac{\partial\tilde{\varphi}(\xi,q)}{\partial\xi} +\frac{N_\mathrm{t}}{N_\mathrm{b}}\frac{\partial^2\tilde{\theta}(\xi,q)}{\partial\xi^2}. \tag{43}$$

We now expand $\tilde{f}(\xi,q)$, $\tilde{g}(\xi,q)$, $\tilde{\theta}(\xi,q)$ and $\tilde{\varphi}(\xi,q)$ by using the Taylor series about $q=0$ as

$$\tilde{f}(\xi,q)=\tilde{f}_0(\xi)+\sum_{m=1}^{\infty}\tilde{f}_m(\xi)q^m;$$
$$\tilde{f}_m(\xi)=\frac{1}{m}\frac{\partial^m\tilde{f}}{\partial q^m}\bigg|_{q=0}, \tag{44}$$
$$\tilde{g}(\xi,q)=\tilde{g}_0(\xi)+\sum_{m=1}^{\infty}\tilde{g}_m(\xi)q^m;$$
$$\tilde{g}_m(\xi)=\frac{1}{m!}\frac{\partial^m\tilde{g}}{\partial q^m}\bigg|_{q=0}, \tag{45}$$
$$\tilde{\theta}(\xi,q)=\tilde{\theta}_0(\xi)+\sum_{m=1}^{\infty}\tilde{\theta}_m(\xi)q^m;$$
$$\tilde{\theta}_m(\xi)=\frac{1}{m!}\frac{\partial^m\tilde{\theta}}{\partial q^m}\bigg|_{q=0}, \tag{46}$$
$$\tilde{\varphi}(\xi,q)=\tilde{\varphi}_0(\xi)+\sum_{m=1}^{\infty}\tilde{\varphi}_m(\xi)q^m;$$
$$\tilde{\varphi}_m(\xi)=\frac{1}{m!}\frac{\partial^m\tilde{\varphi}}{\partial q^m}\bigg|_{q=0}. \tag{47}$$

3.2 *mth-order deformation equations*

The mth-order problems are

$$\mathbf{L}_{\tilde{f}}\big[\tilde{f}_m(\xi)-\chi_m\tilde{f}_{m-1}(\xi)\big]=\hbar_{\tilde{f}}\mathbf{R}^m_{\tilde{f}}(\xi), \tag{48}$$
$$\mathbf{L}_{\tilde{g}}\big[\tilde{g}_m(\xi)-\chi_m\tilde{g}_{m-1}(\xi)\big]=\hbar_{\tilde{g}}\mathbf{R}^m_{\tilde{g}}(\xi), \tag{49}$$
$$\mathbf{L}_{\tilde{\theta}}\big[\tilde{\theta}_m(\xi)-\chi_m\tilde{\theta}_{m-1}(\xi)\big]=\hbar_{\tilde{\theta}}\mathbf{R}^m_{\tilde{\theta}}(\xi), \tag{50}$$
$$\mathbf{L}_{\tilde{\varphi}}\big[\tilde{\varphi}_m(\xi)-\chi_m\tilde{\varphi}_{m-1}(\xi)\big]=\hbar_{\tilde{\varphi}}\mathbf{R}^m_{\tilde{\varphi}}(\xi), \tag{51}$$

$$\tilde{f}_m(0)=\frac{\partial\tilde{f}_m(0)}{\partial\xi}=\frac{\partial\tilde{f}_m(\infty)}{\partial\xi}=0,$$
$$\tilde{\theta}(0)=\tilde{\theta}(\infty)=0,$$
$$\tilde{g}_m(0)=\tilde{g}_m(\infty)=0,$$
$$\tilde{\varphi}(0)=\tilde{\varphi}(\infty)=0, \tag{52}$$

where the functions $\mathbf{R}^m_{\tilde{f}}(\xi)$, $\mathbf{R}^m_{\tilde{g}}(\xi)$, $\mathbf{R}^m_{\tilde{\theta}}(\xi)$ and $\mathbf{R}^m_{\tilde{\varphi}}(\xi)$ are

$$\mathbf{R}^m_{\tilde{f}}(\xi)=\tilde{f}'''_{m-1} +\mathrm{We}\ \mathrm{Re}\Bigg(2\sum_{k=0}^{m-1}\tilde{f}''_{m-1-k}\tilde{f}''_k+\sum_{k=0}^{m-1}\tilde{g}'_{m-1-k}\tilde{g}'_k -2\sum_{k=0}^{m-1}\tilde{f}_{m-1-k}\tilde{f}^{iv}_k+\sum_{k=0}^{m-1}\tilde{f}'_{m-1-k}\tilde{f}'''_k\Bigg) -\mathrm{Re}\Bigg(\sum_{k=0}^{m-1}\tilde{f}'_{m-1-k}\tilde{f}'_k-\sum_{k=0}^{m-1}\tilde{f}_{m-1-k}\tilde{f}''_k -\sum_{k=0}^{m-1}\tilde{g}_{m-1-k}\tilde{g}_k\Bigg)-M\tilde{f}'_{m-1}, \tag{53}$$

$$\mathbf{R}^m_{\tilde{g}}(\xi)=\tilde{g}''_{m-1}+\mathrm{We}\ \mathrm{Re}\Bigg(2\sum_{k=0}^{m-1}f'_{m-1-k}\tilde{g}''_k -2\sum_{k=0}^{m-1}\tilde{f}_{m-1-k}\tilde{g}'''_k-3\sum_{k=0}^{m-1}\tilde{f}''_{m-1-k}\tilde{g}'_k\Bigg) -\mathrm{Re}\Bigg(2\sum_{k=0}^{m-1}\tilde{f}'_{m-1-k}\tilde{g}_k-2\sum_{k=0}^{m-1}\tilde{f}_{m-1-k}\tilde{g}'_k\Bigg) -M\tilde{g}_{m-1}, \tag{54}$$

$$\mathbf{R}^m_{\tilde{\theta}}(\xi)=\tilde{\theta}''_{m-1}+2\mathrm{Re}\,\mathrm{Pr}\sum_{k=0}^{m-1}\tilde{f}_{m-1-k}\tilde{\theta}'_k +\mathrm{Re}\ \mathrm{Pr}\,Q\sum_{k=0}^{m-1}\tilde{\theta}_{m-1}+N_\mathrm{b}\,\mathrm{Pr}\sum_{k=0}^{m-1}\tilde{\theta}'_{m-1-k}\tilde{\varphi}'_k +N_\mathrm{t}\,\mathrm{Pr}\sum_{k=0}^{m-1}\tilde{\theta}'^2_{m-1} +M\,\mathrm{Pr}\,\mathrm{Ec}\sum_{k=0}^{m-1}\Big(\tilde{f}'^2_{m-1-k}+g^2_{m-1-k}\Big) +R_d\Bigg(3(\theta_w-1)\Big(\tilde{\theta}'^2_{m-1} +\sum_{k=0}^{m-1}\tilde{\theta}^2_{m-1-k}\tilde{\theta}'^2_k(\theta_w-1)^2 +2\sum_{k=0}^{m-1}\tilde{\theta}_{m-1-k}\tilde{\theta}'^2_k(\theta_w-1)\Bigg)+\tilde{\theta}''_{m-1}$$

$$+(\theta_w-1)^3\sum_{k=0}^{m-1}\tilde{\theta}^3_{m-1-k}\tilde{\theta}''_k$$
$$+3(\theta_w-1)\sum_{k=0}^{m-1}\tilde{\theta}_{m-1-k}\tilde{\theta}''_k$$
$$+3\sum_{k=0}^{m-1}(\theta_w-1)^2\tilde{\theta}^2_{m-1-k}\tilde{\theta}''_k\Bigg), \tag{55}$$

$$\mathbf{R}^m_{\tilde{\varphi}}(\xi)=\tilde{\varphi}''_{m-1}+2\text{Re Sc}\sum_{k=0}^{m-1}\tilde{f}_{m-1-K}\tilde{\varphi}'_K+\frac{N_\text{t}}{N_\text{b}}\tilde{\theta}''_{m-1}, \tag{56}$$

$$\chi_m=\begin{cases}0, & m\le 1,\\ 1, & m>1.\end{cases} \tag{57}$$

The general solutions can be written as

$$\tilde{f}_m(\xi)=\tilde{f}^*_m(\xi)+c_1+c_2\mathrm{e}^{-\xi}+c_3\mathrm{e}^{\xi}, \tag{58}$$
$$\tilde{g}_m(\xi)=\tilde{g}^*_m(\xi)+c_4\mathrm{e}^{-\xi}+c_5\mathrm{e}^{\xi}, \tag{59}$$
$$\tilde{\theta}_m(\xi)=\tilde{\theta}^*_m(\xi)+c_6\mathrm{e}^{-\xi}+c_7\mathrm{e}^{\xi}, \tag{60}$$
$$\tilde{\varphi}_m(\xi)=\tilde{\varphi}^*_m(\xi)+c_8\mathrm{e}^{-\xi}+c_9\mathrm{e}^{\xi}, \tag{61}$$

where the constants c_i $(i=1-9)$ by using the boundary conditions (52) have the values

$$c_1=-c_2-\tilde{f}^*_m(0),\quad c_2=\frac{\partial\tilde{f}^*_m(0)}{\partial\xi},$$
$$c_4=-\frac{\partial\tilde{g}^*_m(0)}{\partial\xi},\quad c_6=-\frac{\partial\tilde{\theta}^*_m(0)}{\partial\xi},$$
$$c_8=-\frac{\partial\tilde{\varphi}^*_m(0)}{\partial\xi},\quad c_3=c_5=c_7=c_9=0. \tag{62}$$

4. Convergence analysis

With the help of auxiliary parameters $\hbar_{\tilde{f}}$, $\hbar_{\tilde{g}}$, $\hbar_{\tilde{\theta}}$ and $\hbar_{\tilde{\varphi}}$, we can regulate the convergence region. By using the homotopy analysis method (HAM), we can solve the system of equations. Figure 2 shows the $\hbar$-curves at the 25th order of deformation. Convergence regions for these parameters are $-2\le\hbar_{\tilde{f}}\le-1$, $-2\le\hbar_{\tilde{g}}\le-0.1$, $-2\le\hbar_{\tilde{\theta}}\le-0.5$ and $-1.5\le\hbar_{\tilde{\varphi}}\le-0.5$. Table 1 demonstrates the convergence order for $\tilde{f}''(0)$, $\tilde{g}'(0)$, $\tilde{\theta}'(0)$ and $\tilde{\varphi}'(0)$ which converges at the 12th, 11th, 28th and 28th order of approximations, respectively.

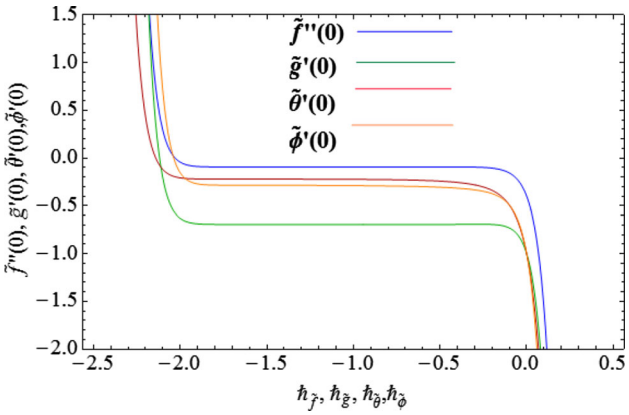

Figure 2. h curve at $\tilde{f}''(0)$, $\tilde{g}'(0)$, $\tilde{\theta}'(0)$ and $\tilde{\varphi}'(0)$.

Table 1. Solution convergence occurs when Re = 0.3, We = 0.01, R_d = 0.01, θ_w = 0.1, A = 0.4, Pr = 1.5, Q = 0.01, Ec = 0.4, Sc = 1, N_b = 0.3, N_t = 0.01, M = 0.2.

Order of approximation	$-\tilde{f}''(0)$	$-\tilde{g}'(0)$	$-\tilde{\theta}'(0)$	$-\tilde{\varphi}'(0)$
1	0.05554	0.5800	0.5713	0.5233
12	0.09494	0.6942	0.2365	0.3021
17	0.09494	0.6942	0.2277	0.2939
24	0.09494	0.6942	0.2235	0.2890
27	0.09494	0.6942	0.2228	0.2879
28	0.09494	0.6942	0.2226	0.2877

5. Results and discussion

In this section, the behaviour of influential variables on velocity, temperature, concentration, coefficients of skin friction and the Nusselt number is analysed. In figures 3–23, we fixed We = 0.3, Re = 0.9 = 0.9 = 0.7, Ec = 0.4, Q = 0.7, N_t = 0.3, N_b = 0.3, R_d = 0.5, θ_w = 0.2, Sc = 1 and M = 0.5.

5.1 *Dimensionless velocities*

Figures 3–10 illustrate the velocities of various parameters. In figures 3 and 4, the effects of viscoelastic parameter (ξ) (when We = 0, 0.4, 0.8, 1.2) on axial $(\tilde{f}(\xi))$ and radial $(\tilde{f}'(\xi))$ velocities are shown. We know that the Weissenberg number (We) is inversely proportional to the fluid viscosity because of which the motion of the fluid increases with larger We. The effect of the Reynolds number Re on $(\tilde{f}(\xi), \tilde{g}(\xi))$ is shown in figures 5 and 6. Here, for increasing values of the Reynolds number (Re) (Re = 0, 0.5, 1, 1.5), $(\tilde{f}(\xi), \tilde{g}(\xi))$ decreases because inertial forces become stronger for higher Re. The behaviour of velocities $(\tilde{f}(\xi), \tilde{g}(\xi))$ for the stretching parameter (A) is

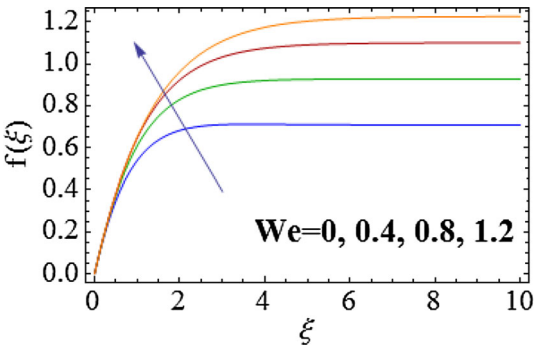

Figure 3. Graph of $f(\xi)$ against We.

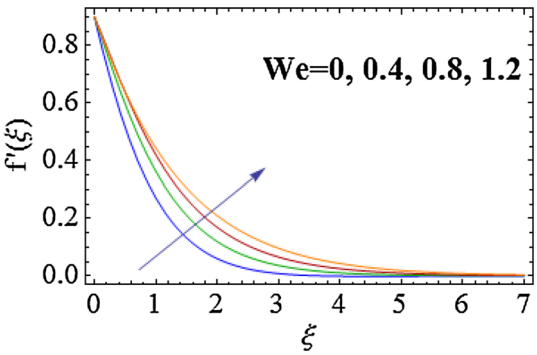

Figure 4. Graph of $f'(\xi)$ against We.

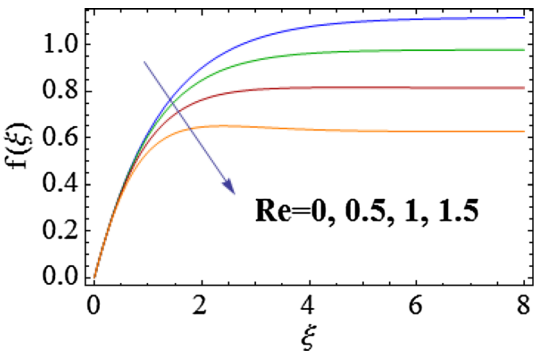

Figure 5. Graph of $f(\xi)$ against Re.

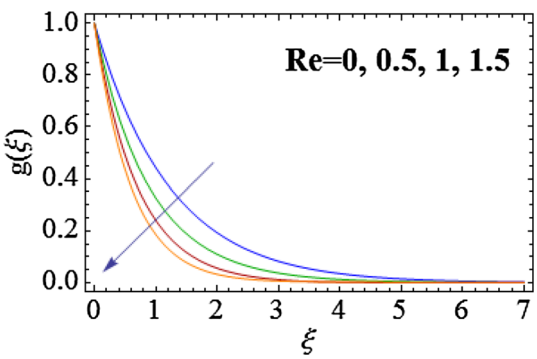

Figure 6. Graph of $g(\xi)$ against Re.

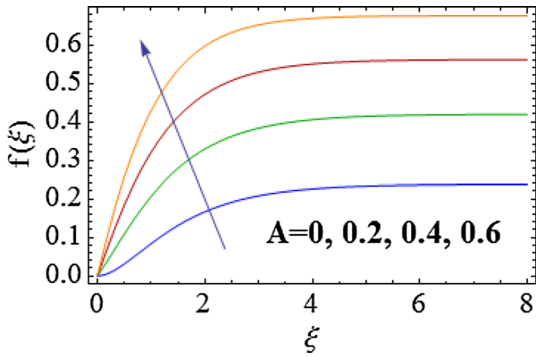

Figure 7. Graph of $f(\xi)$ against A.

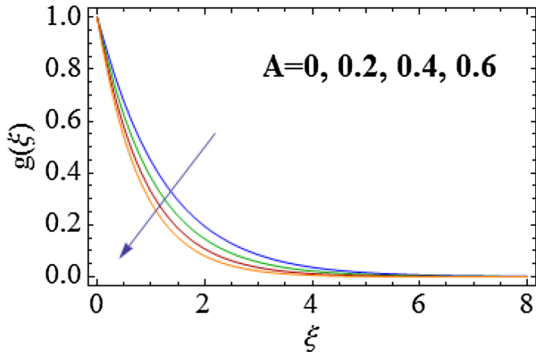

Figure 8. Graph of $g(\xi)$ against A.

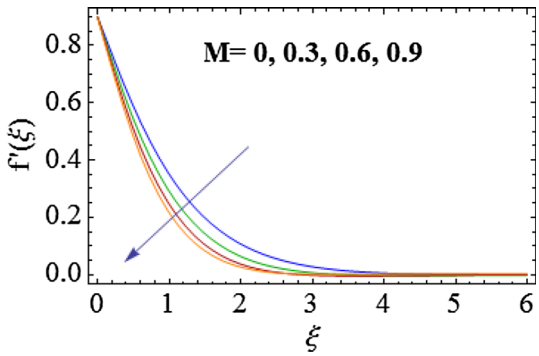

Figure 9. Graph of $f'(\xi)$ against M.

discussed in figures 7 and 8. For larger values of A ($A = 0,\ 0.2,\ 0.4,\ 0.6$), momentum boundary layer and $\tilde{f}(\xi)$ rise for a longer stretching rate (see figure 7). On the other hand, the reverse trend is noticed for $\tilde{g}(\xi)$ because the angular velocity (Ω_1) reduces. Figures 9 and 10 show the effect of magnetic parameter M on $\left(\tilde{f}'(\xi), \tilde{g}(\xi)\right)$. We know that the Lorentz force is related to the magnetic field which causes resistance to the flow, and so $\left(\tilde{f}'(\xi),\ \tilde{g}(\xi)\right)$ reduces for M.

5.2 *Temperature*

The analysis of temperature distribution $\tilde{\theta}(\xi)$ against different parameters is deliberated in figures 11–16. The

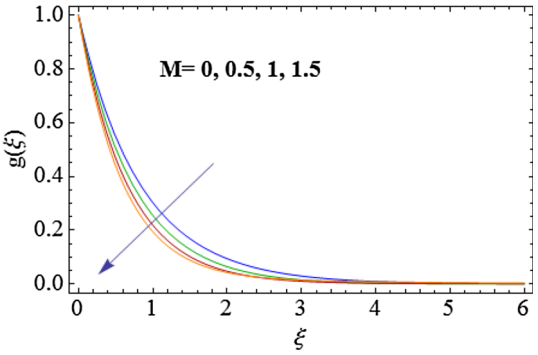

Figure 10. Graph of $g(\xi)$ against M.

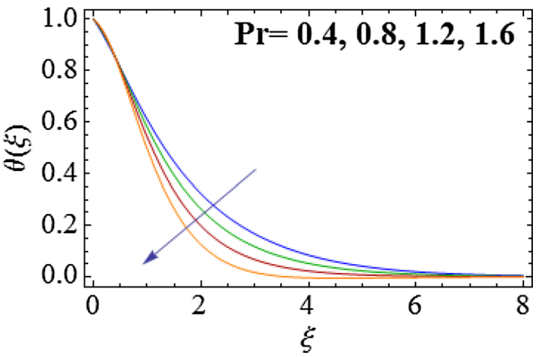

Figure 11. Graph of $\theta(\xi)$ against Pr.

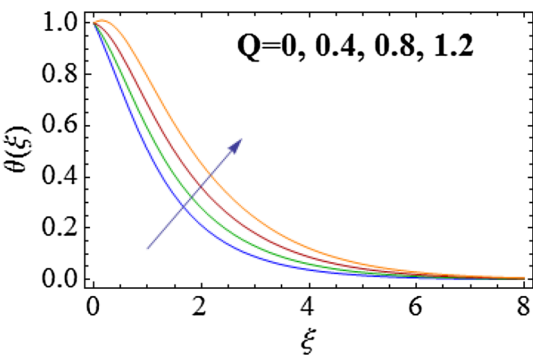

Figure 12. Graph of $\theta(\xi)$ against Q.

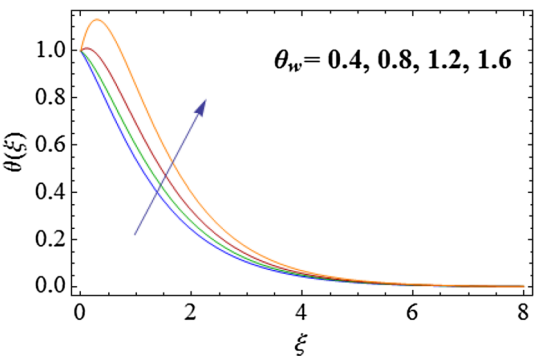

Figure 13. Graph of $\theta(\xi)$ against θ_w.

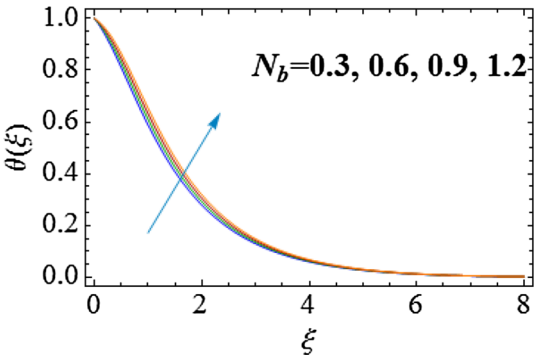

Figure 14. Graph of $\theta(\xi)$ against N_{b}.

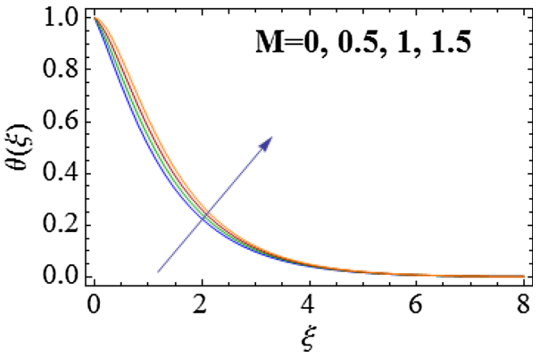

Figure 15. Graph of $\theta(\xi)$ against M.

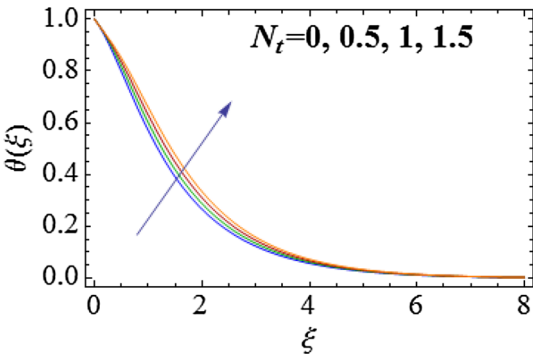

Figure 16. Graph of $\theta(\xi)$ against N_{t}.

behaviour of Pr with $\tilde{\theta}(\xi)$ is discussed in figure 11. As Pr is inversely proportional to thermal diffusivity, for large values of Pr (Pr $=$ 0.4, 0.8, 1.2, 1.6), the temperature of the fluid decreases. The effect of Q on the temperature is shown in figure 12. Clearly, $\tilde{\theta}(\xi)$ boosts up for larger Q ($Q = 0, 0.4, 0.8, 1.2$) because heat generation/absorption coefficient increases. Figure 13 demonstrates the behaviour of $\tilde{\theta}(\xi)$ against θ_w. The thermal state of the fluid enhances by increasing θ_w (θ_w $=$ 1.1, 1.3, 1.5, 1.7) due to which the temperature is enhanced. Figure 14 illustrates the effect of N_{b} on $\tilde{\theta}(\xi)$. Temperature increases for higher N_{b}. Figure 15 shows the behaviour of the magnetic field

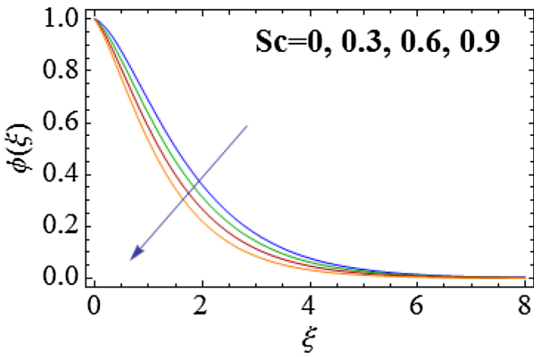

Figure 17. Graph of $\varphi(\xi)$ against Sc.

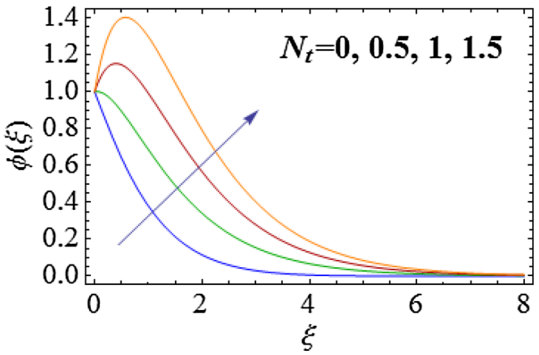

Figure 18. Graph of $\varphi(\xi)$ against N_{t}.

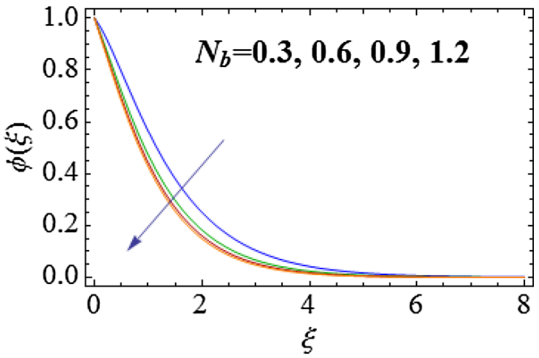

Figure 19. Graph of $\varphi(\xi)$ against N_{b}.

(M) on temperature distribution. An increase in M $(M = 0, 0.5, 1, 1.5)$ gives rise to $\tilde{\theta}(\xi)$. It is for larger Lorentz force. In figure 16, both $\tilde{\theta}(\xi)$ and the thermal layer thickness are increased for $N_{\mathrm{t}} = 0, 0.5, 1, 1.5$. An enhancement in N_{t} results in a stronger thermophoretic force due to which nanoparticles are transferred from warm to cold regions, and hence $\tilde{\theta}(\xi)$ rises.

5.3 *Concentration*

The behaviour of the concentration is portrayed in figures 17–19. The influence of the Schmidt number (Sc) on $\tilde{\varphi}(\xi)$ is described in figure 17. Large values of Sc $(\mathrm{Sc} = 0, 0.3, 0.6, 0.9)$ decrease the concentration.

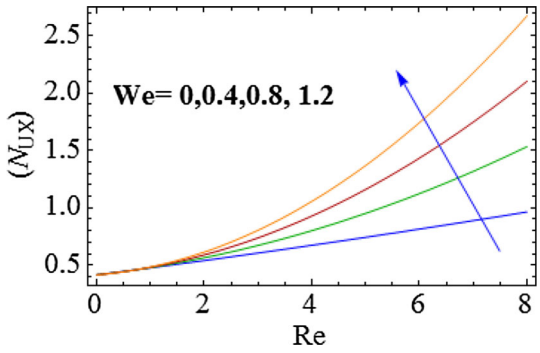

Figure 20. Graph of Nu_x against We.

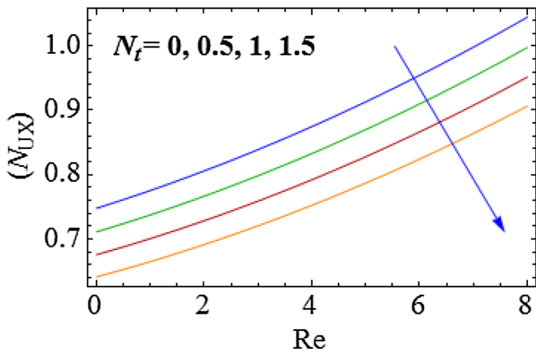

Figure 21. Graph of Nu_x against N_{t}.

In fact, higher values of Sc result in low molecular diffusivity. The impacts of N_{t} and N_{b} on $\tilde{\varphi}(\xi)$ are shown in figures 18 and 19. With an enhancement of $N_{\mathrm{t}} = 0, 0.5, 1, 1.5$, thermophoresis force rises. Such force tends to move nanoparticles from warm to cold regions and hence $\tilde{\varphi}(\xi)$ rises. Moreover, the concentration layer thickness is also enhanced for larger N_{t}. The higher the values of N_{b} $(N_{\mathrm{b}} = 0.3,\ 0.6,\ 0.9,\ 1.2)$, the smoother is the distribution of nanoparticles concentration in the fluid system, which eventually decreases $\tilde{\varphi}(\xi)$.

5.4 *Nusselt number*

Figures 20 and 21 demonstrate the effect of the viscoelastic parameter (We) and the thermophoresis parameter (N_{t}) on the rate of heat transfer. These figures show that the Nusselt number increases for higher values of We while a reverse behaviour is noticed for N_{t}.

5.5 *Skin friction coefficients*

Figures 22 and 23 indicate the effects of A and We on the skin friction coefficients. Here, the magnitude of the surface drag force in radial and tangential directions is more for larger A and We.

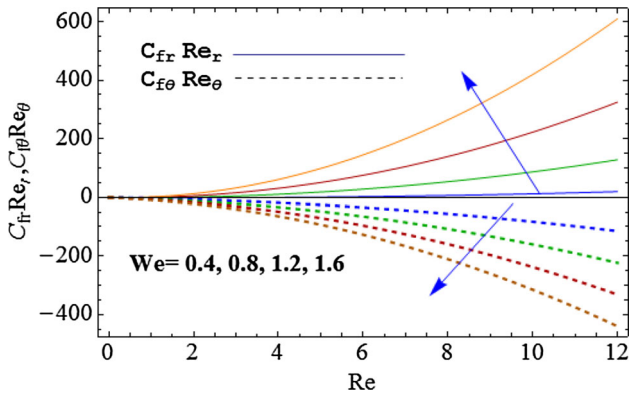

Figure 22. Graph of Cf_r Re$_r$ and Cf_θ Re$_\theta$ against We.

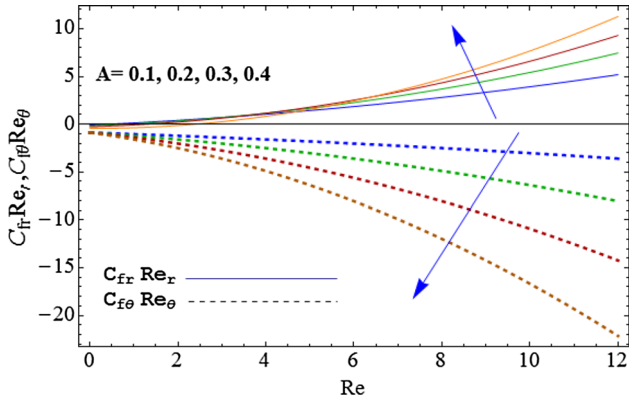

Figure 23. Graph of Cf_r Re$_r$ and Cf_θ Re$_\theta$ against A.

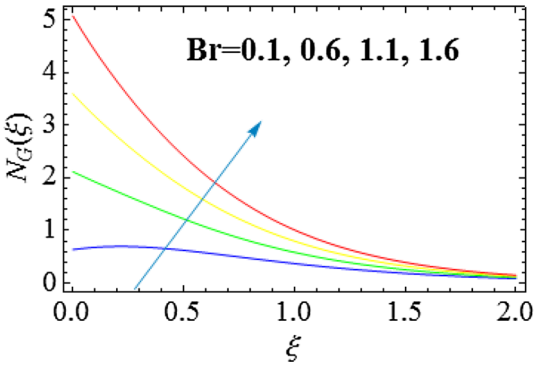

Figure 24. Graph of N_G against Br.

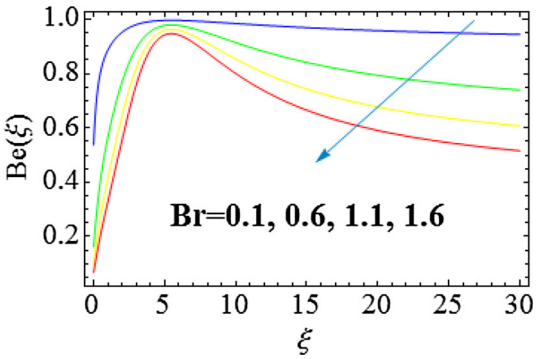

Figure 25. Graph of Be against Br.

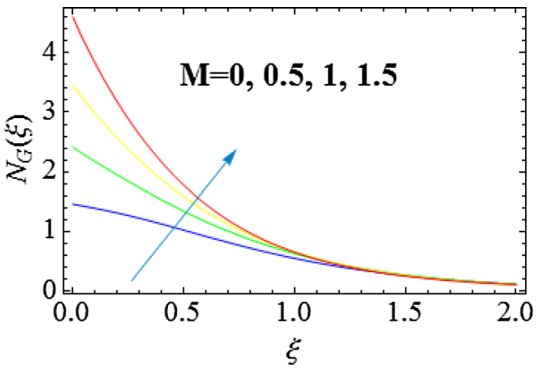

Figure 26. Graph of N_G against M.

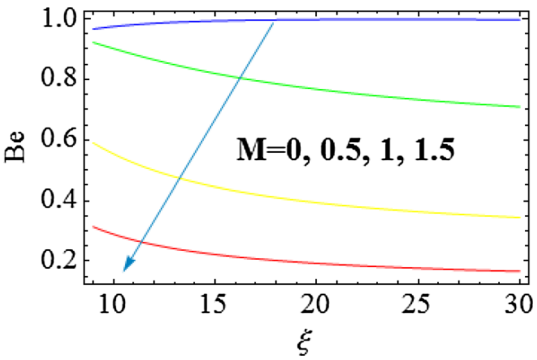

Figure 27. Graph of Be against M.

5.6 *Entropy generation and Bejan number*

Figures 24–33 illustrate the trends of N_G and Be for different parameters. Figures 24 and 25 show the behaviour of N_G and Be on the Brinkman number (Br). Br is associated with the heat transfer from a disk to the flow of a viscous fluid. Figure 24 indicates more entropy generation rate for larger Br because by dissipation, the conduction rate is slowly created. Figure 25 shows the behaviour of Br on Be as entropy generation is more for large Br. It means viscosity is dominant over heat transfer irreversibility, and hence Be decreases. In figures 26 and 27, the influence of the magnetic variable (M) on N_G and Be is noticed. In figure 26, the entropy generation rate is addressed for large values of M. The entropy generation rate is enhanced for large M because drag force is higher for larger M. Figure 27 shows the decaying behaviour of Be for a larger magnetic variable M. Figures 28 and 29 describe the behaviour of the diffusion parameter (L^*) on N_G and Be. It is noticed that for L^*, both N_G and Be are increasing functions. The diffusion rate of nanoparticles enhances for larger L^*. That is why the total entropy of the system and Be are enhanced. Figures 30 and 31 show the impact of θ_w on N_G and Be. Here, both N_G and Be are increasing functions of θ_w. As

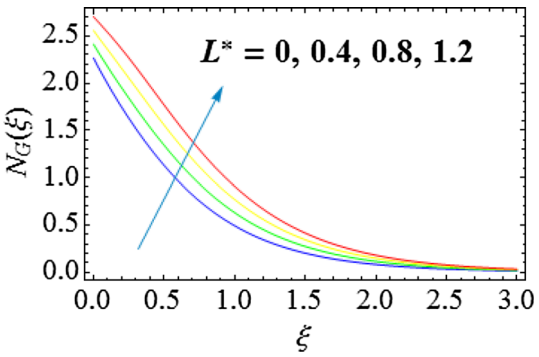

Figure 28. Graph of N_G against L^*.

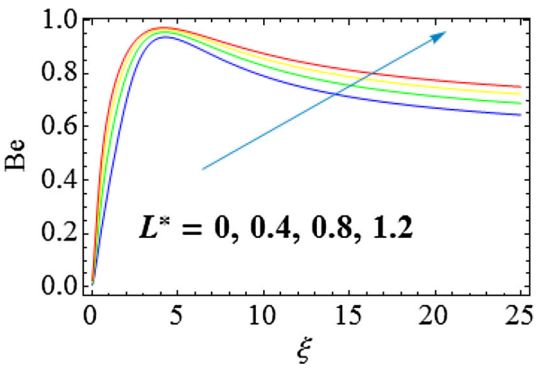

Figure 29. Graph of Be against L^*.

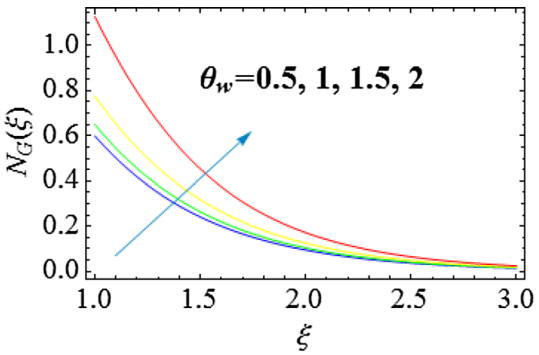

Figure 30. Graph of N_G against θ_w.

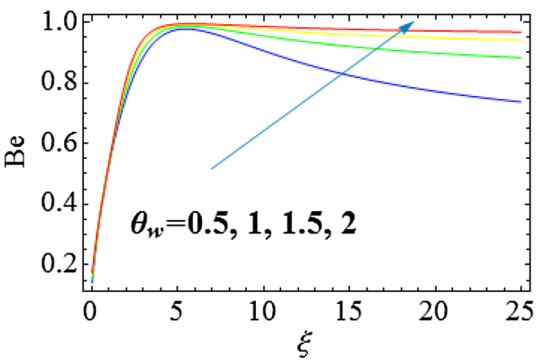

Figure 31. Graph of Be against θ_w.

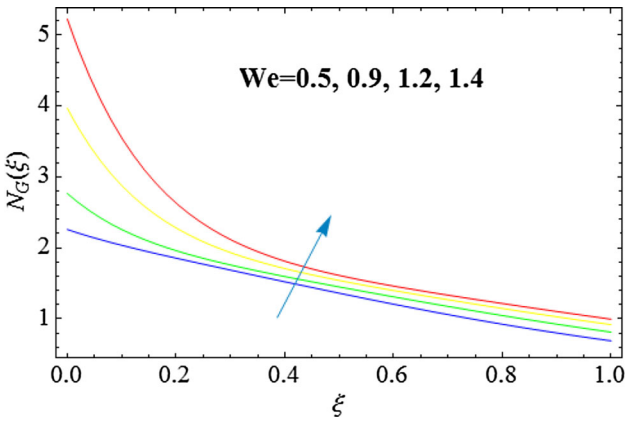

Figure 32. Graph of N_G against We.

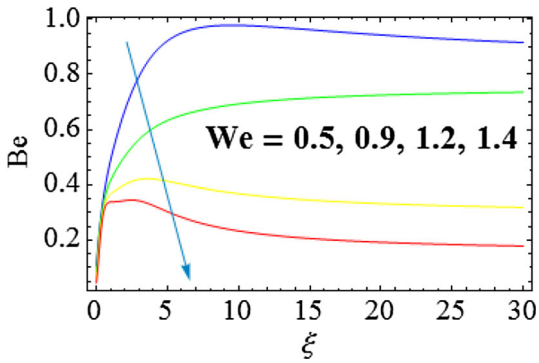

Figure 33. Graph of Be against We.

the disk is heated, for larger values of the temperature ratio (θ_w), the disorderedness near the disk is high and so N_G increases (see figure 30). Here, the irreversibility of the mass and heat transfer prevail over the irreversibility of the friction of the fluid for higher θ_w, and so Be also rises (see figure 31). Trends of N_G and Be vs. We are displayed in figures 32 and 33. Disorderedness in the system is more for larger We (see figure 32). Be decays for increasing We (see figure 33).

6. Conclusions

Major findings of this study are:

- For larger viscoelastic parameter (We), the velocities (radial ($\tilde{f}(\xi)$), axial ($\tilde{f}'(\xi)$) and tangential ($\tilde{g}(\xi)$)) are increased.
- Temperature ($\tilde{\theta}(\xi)$) against θ_w, N_t, M and Q enhances.
- Concentration reduces for A, N_b, Re and Sc.
- Entropy generation (N_G) enhances for We and Br while the opposite trend is noticed against We.
- Both N_G and Be are enhanced for larger L^* and θ_w.

Acknowledgements

The authors are grateful to the Higher Education Commission (HEC) of Pakistan for financial support to this work under Project No. 20-3038/NRPU/R&D/HEC/13.

References

[1] S U S Choi, *ASME Fed.* **66**, 99 (1995)
[2] M Farooq, M I Khan, M Waqas, T Hayat, A Alsaedi and M I Khan, *J. Mol. Liq.* **221**, 1097 (2016)
[3] M Sajid, S A Iqbal, M Naveed and Z Abbas, *J. Mol. Liq.* **233**, 115 (2017)
[4] K Sreelakshmi and G Sarojamma, *Trans. A. Razm. Math. Int.* **172**, 606 (2018)
[5] S Saranya, P Ragupathi, B Ganga, R P Sharma and A K A Hakeem, *Adv. Powder Technol.* **29**, 1977 (2018)
[6] P Sreedevi, P S Reddy and A J Chamkha, *Powder Technol.* **315**, 194 (2017)
[7] S Qayyum, M I Khan, T Hayat and A Alsaedi, *Results Phys.* **7**, 1907 (2017)
[8] Z Abbas and M Sheikh, *Chin. J. Chem. Eng.* **25**, 11 (2017)
[9] T Hayat, M I Khan, S Qayyum and A Alsaedi, *Colloids Surf. A* **539**, 335 (2018)
[10] T Hayat, S Qayyum, M Imtiaz and A Alsaedi, *Int. J. Heat Mass Transf.* **102**, 723 (2016)
[11] T Hayat, I Ullah, B Ahmed and A Alsaedi, *Results Phys.* **7**, 2804 (2017)
[12] Z A Zaidi and S T Mohyud-Din, *J. Mol. Liq.* **230**, 230 (2017)
[13] A A Afify and N S Elgazery, *Particuology* **29**, 154 (2016)
[14] M Mustafa, *Int. J. Heat Mass Transf.* **113**, 1012 (2017)
[15] T Hayat, S Nawaz, A Alsaedi and M Rafiq, *Results Phys.* **7**, 982 (2017)
[16] M I Khan, S Qayyum, T Hayat, M I Khan and A Alsaedi, *Results Phys.* **7**, 3968 (2017)
[17] T Hayat, S Qayyum, M Imtiaz and A Alsaedi, *Results Phys.* **7**, 2557 (2017)
[18] T Hayat, S Qayyum, A Alsaedi and B Ahmad, *Results Phys.* **8**, 223 (2018)
[19] F M Abbasi, S A Shehzad, T Hayat and B Ahmad, *J. Magn. Magn. Mater.* **404**, 159 (2016)
[20] S Qayyum, T Hayat, M I Khan, M I Khan and A Alsaedi, *J. Mol. Liq.* **262**, 261 (2018)
[21] V L Berdichevsky, *Int. J. Eng. Sci.* **128**, 24 (2018)
[22] M I Khan, S Qayyum, T Hayat, M Waqas, M I Khan and A Alsaedi, *J. Mol. Liq.* **259**, 274 (2018)
[23] Y Haseli, *Energy Convers. Manage.* **159**, 109 (2018)
[24] T Hayat, M I Khan, S Qayyum, A Alsaedi and M I Khan, *Phys. Lett. A* **382(11)**, 749 (2018)
[25] C Jia, R Zeng, X Peng, L Zhang and Y Zhao, *Chem. Eng. Sci.* **190**, 1 (2018)
[26] C S Jia, C W Wang, L H Zhang, X L Peng, H M Tang, J Y Liu, Y Xiong and R Zeng, *Chem. Phys. Lett.* **692**, 57 (2018)
[27] C S Jia, C W Wang, L H Zhang, X L Peng, H M Tang and R Zeng, *Chem. Eng. Sci.* **183**, 26 (2018)
[28] X L Peng, R Jiang, C S Jia, L H Zhang and Y L Zhao, *Chem. Eng. Sci.* **190**, 122 (2018)
[29] S Qayyum, M I Khan, T Hayat, A Alsaedi and M Tamoor, *Int. J. Heat Mass Transf.* **127**, 933 (2018)
[30] M Turkyilmazoglu, *Math. Comput. Model.* **53**, 1929 (2011)
[31] T Hayat, S Qayyum, M I Khan and A Alsaedi, *AIP Phy. Fluids* **30**, 017101 (2018)
[32] S Abbasbandy and T Hayat, *Commun. Nonlinear Sci. Numer. Simul.* **14**, 3591 (2009)
[33] L Zheng, L Wang and X Zhang, *Commun. Nonlinear Sci. Numer. Simul.* **16**, 731 (2011)
[34] T Hayat, M I Khan, S Qayyum and A Alsaedi, *Chin. J. Phys.* **55**, 2501 (2017)
[35] T Hayat, K Muhammad, M I Khan and A Alsaedi, *Pramana – J. Phys.* **92**: 57 (2019)